PHYSICAL REVIEW C VOLUME 12, NUMBER 6 DECEMBER 1975

Longitudinal electron polarization for a second-forbidden beta decay

Duane R. Doty
California State University, Northridge, Northridge, California 91324

Earle I. Neill, Jr.
Hughes Airfcraft Corporation, Albuquerque, New Mexico 87115
(Received 16 June 1975)

Electron polarization from the second-forbidden β decay in ^{137}Cs has been investigated by use of a lens spectrometer. Møller scattering from a hydrogen-annealed Supermendur foil of 2×10^{-2} mm thickness was employed to measure the polarization. Fast-slow coincidence techniques were used. Solid state detectors, a small area scattering foil, and a highly collimated spectrometer defined the scattering geometry and helped to reduce background. Analysis of the data was performed from a two-parameter recording to eliminate chance coincidence events. Two independent techniques of measurement resulted in $P_e = -1.0 \pm 0.2$. A substantial deviation from the value of $P_e = -v/c = 0.92$, which would be expected for allowed decays, was not observed.

[RADIOACTIVITY ^{137}Cs; Møller scattering, measured electron polarization of second-forbidden decay.]

I. INTRODUCTION

For allowed β decays the two-component neutrino theory of Feynman,[1] Konopinski,[2] and Gell-Mann[3] predicts that the helicity of emitted electrons is $P = -v/c$. This prediction has been verified by numerous investigators.[4-10] Very little work has been published on second-forbidden transitions. It was pointed out by Schopper[11] that these transitions ought to be investigated because the resulting experimental data might give information on nuclear matrix elements.

The work reported in this paper pertains to helicity measurements on the β transition at 1.176 MeV in ^{137}Cs. This is a transition known to be of the forbidden type.[12] In the vicinity of this transition intense electron emission takes place from other branches of decay; therefore a highly selective experimental procedure is required to separate the events resulting from this weak transition from other events of nearly equal energy.

II. EXPERIMENTAL METHOD

Møller scattering was chosen among the many experimental techniques available because of the relative efficiency at the energies studied, the experimental simplicity, and the complete theoretical calculations which exist with small correction factors. The technique, which is amply described in the textbook literature[7,13,14] requires the focusing of a portion of the electron beam on a polarized target and the observation of the scattered electrons by means of two detectors.

The Møller-scattering cross section has its greatest dependence on the relative spin orientation of incident and target electrons when the incident electron transfers half of its kinetic energy to the target electron. Then, nonrelativistic collision theory predicts scattered electrons will emerge at equal angles, ϕ, of 45° each with respect to the incident electron's momentum, as is shown in Fig. 1. A relativistic calculation at the energy in question reduces ϕ to 36°. The angle θ defines the incident electron's momentum vector with respect to the B vector of the polarized target. The two outgoing electrons are counted in coincidence. With the constraints of angle, energy, and time placed on the accepted events background scattering, due mainly to Coulomb scattering, is effectively suppressed.

The magnetic polarization in the foil must be reversed to obtain comparison coincidence rates for parallel and antiparallel spin electron-electron scattering. This change will alter the incoming β ray trajectories in a manner difficult to compensate for. Previous experimental techniques have employed large transmission spectrometers and large detector apertures. Accurate definition of the electron trajectories becomes even more difficult. The present apparatus represents an improvement in resolution which defines the scattering angle ϕ more precisely. A smaller transmission spectrometer was employed to limit the variance $\Delta\theta$ in the incident solid angle on the target. These refinements reduce chance coincidence and multiple scattering events and remove the necessity of averaging over angular variables in the calculations.

The angle θ is largely determined by spectrometer construction and $\Delta\theta$ is minimized by collimation near the source region. Measurement of

θ was first performed photographically and resulted in $\theta = 18.5° \pm 2°$. Detector position θ with respect to the trajectory was made variable and the angle θ was later verified to be 18.5° independently by the use of coincident count rates versus detection angle. After these measurements the detectors were set symmetrically at $\phi = 36°$ each and remained fixed.

A polarizable target 2×10^{-2} mm thick of Supermendur foil was constructed of dimensions 5 mm $\times$5 mm. Hydrogen-annealed Supermendur[15] has a coercive force of 0.26 Oe and a maximum permeability of 66 000 at 20 000 G. This target was suspended in the scattering geometry by fine silk threads so that all of the foil was seen by the detectors. The low Z and very small size of target support is estimated to contribute less than one-half of 1% to the scattering electrons present and this fraction is, of course, not polarizable.

Solid-state lithium-drifted silicon detectors of 2000 μm depletion depths were used. Their active surface areas for detection are 25 mm^2 each. Their size in turn limited the precision of the scattering angles to a $\Delta\phi$ of $\pm 5°$. Brass collimators were constructed to limit the view of each detector to the target region only. Neither detector could see the collimator of the other. A variable detector mounting (adjustment outside the spectrometer's vacuum tank) enabled alteration of the θ and ϕ angles so that with templates angle measurements could be made with an accuracy of $\pm 2°$.

A sliding target holder enabled the removal of the polarized target from the scattering region. A second aluminum target of similar size and thickness can be introduced to the scattering region to provide a nonpolarizable electron-electron scattering. Additionally, it was possible to remove all scattering foils and observe background and collimator scattering.

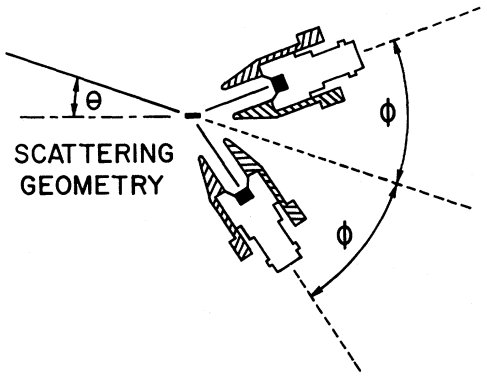

FIG. 1. Electron-electron scattering geometry. Dark straight lines represent electron trajectories. θ defines the incident electron beam with respect to the target's plane of polarization. ϕ is the scattering angle with respect to the incident electron trajectory.

The electron source was made of high specific activity cesium nitrate deposited on a stainless-steel foil of 2.5×10^{-3} mm thickness and covered by a similar foil. A total activity of 50 mc. was confined to a source size of approximately 3 mm in diameter and an average thickness of 0.6 mg/cm^2.

Lead, brass, and aluminum collimators at the source end of the spectrometer limited radiation to a thin conical region of 10° angular width. Transmission of 4% was measured for this geometry. Since the electrons underwent an azimuthal angular collimation as well, only 0.2% of the emitted electrons reached the target.

Figure 2 shows an upper view and a side view of the lens spectrometer. In this configuration of a magnetic field the electron trajectories are helical. With collimation and a specific current direction in the lens coils a well-defined helical electron trajectory was established and its properties measured both by detector position movement and by photographic methods. When the lens current is reversed a helix of opposite pitch is produced but with the same entrance angle θ upon the target. These beams may not be of the same intensities because the source may not be fully isotropic, but their difference is readily measurable.

Figure 3 shows an end view of these two trajectories. Note the large amount of lead, about 90 cm in length, which was placed between the source and detectors to cut down chance coincidence events.

The reversal of the spectrometer's field automatically reverses polarization of the target and results in negligible perturbation of the electron's trajectory due to the presence of the scattering foil. Electrons of identical energies are focused for both current polarities since the spectrometer is virtually iron free. A current regulated power supply was used to maintain accurate momentum discrimination over the long-recording times needed which totaled over 11 months.

III. DATA ACQUISITION

Output pulses were obtained from the detectors by requiring a fast coincident overlap of between 20 to 100 nsec. Faster times were not obtainable because of the relative slow collection time for the rather thick depletion regions in the detectors. Coincident pulses were then stored in a 1024

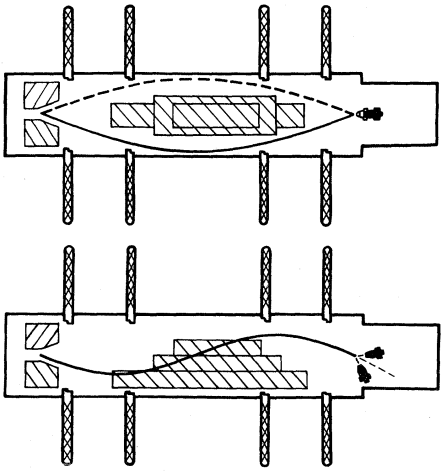

FIG. 2. The upper figure shows a top view of the lens spectrometer. Four current coils are shown cut away from the central vacuum chamber. Some of the lead shielding is shown on the left (source) end and in the central region. The detectors are visible at the right end. A solid line represents an allowed electron trajectory for particular current direction in the lens coils. The dotted line is the allowed trajectory for the current reversed in the coils. Below is a side view.

channel analyzer in the multiparameter mode to produce a 32×32 channel array. The detector at room temperature had a resolution of 10% at 800 keV. With such resolution a 32 channel display was adequate. Paper-tape printouts were acquired each day and a new set of data was generated. Because of the low coincidence rates, in the order of only one event every several minutes, hundreds of tapes were generated over a typical recording period of several months. The printout of each run was visually analyzed. This was necessary because otherwise occasionally occurring power transients could have introduced easily recognizable but erroneous data into the analyzer's memory.

A typical spectrum obtained with 40 nsec fast-slow coincidence summed over 30 days is shown in Fig. 4. The incident electron energy of 780 keV can be seen as a chance coincidence peak in the lower right of the graph. The large true coincidence Møller scattering at 390 keV is shown in the graph's central region. Its symmetric and well-defined shape indicates an appropriately defined scattering geometry. Due to the target's finite size the resolution of the monochromator amounted to 8 keV at about 780 keV. Symmetry in the observed Møller spectrum was a further check used to define detector positions and the scattering angles. Resolution of the main peak is mainly limited by detector resolution. Low energy valleys indicate the lack of multiple scatterings events which would contribute to depolarization corrections. Figure 4 represents over 10 000 coincident events in the half energy Møller scattering peak for a particular polarization of the scattering foil. For analysis, altogether six times this amount of data is needed representing over one year of acquisition time. From day to day, the polarization was reversed to build up

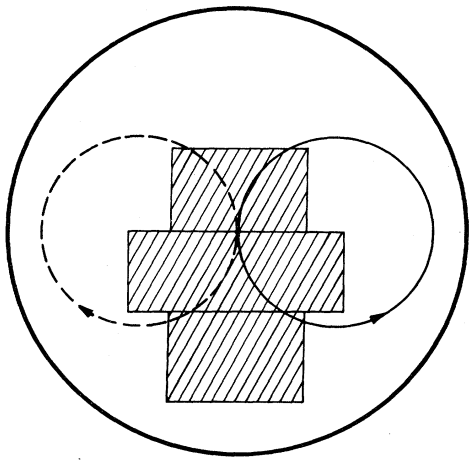

FIG. 3. An end view of the spectrometer chamber showing central lead shielding and the two allowed helical trajectories for the two current directions in the magnetic lenses.

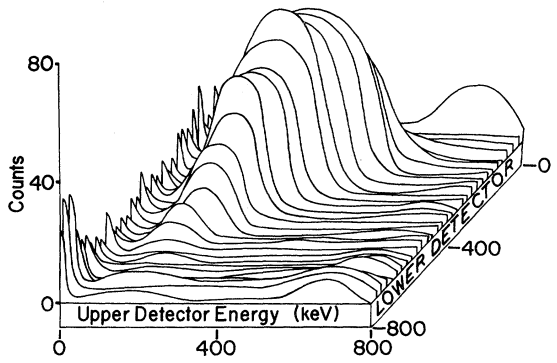

FIG. 4. A Møller scattering spectrum summed over 30 days. The incident electron energy is 780 keV. The lower right peak is chance coincidence. The symmetric central peak is true coincidence events riding on a chance coincidence continuum.

statistics evenly for parallel and antiparallel scatterings.

IV. ANALYSIS OF THE DATA

For a particular energy observation six types of data sets were taken. These consisted of iron scattering, aluminum scattering, and background scattering. Each of these in turn was recorded for both polarization directions. Visual analysis of each run and a computer contour plot enabled removal of transient containing data runs. An additional program added accepted data for storage and integrated the total events under an area corresponding to acceptable energies for Møller scattering. After a run was ascertained to be acceptable, only three numbers were of importance, the areas under the true and chance coincidence peaks and the live time recorded for the run.

A chance coincidence run would look like Fig. 4 without the large central true coincidence hill. The number of events under the coincidence area may be considerable and for a background run the true-to-chance area ratio was uniquely determined by summing and comparing data in the two regions. Once this ratio was found for a given polarization (solenoid current) direction, background could be subtracted from the aluminum and iron data unambiguously by simply measuring the events in their respective chance peaks and then applying the ratio. In this manner C, the true coincidence count rate for aluminum or the Supermendur foil, was determined. Since aluminum is nonpolarizable, a determination of the true coincidence counting rates for the two current directions C_+ or C_- will be the same as the ratio of the two helical beam intensities associated with the current changes in the lens spectrometer. With this additional ratio the Supermendur data were corrected for background and intensity variations.

Polarization of the incident electron is found[7] from

$$P_e = \frac{\delta}{2f\cos\theta R},$$

where δ equals $2(C_+ - C_-)/(C_+ + C_-)$ with + (−) implying parallel (antiparallel) electron-electron scattering, f equals the fraction of aligned electrons in the Supermendur foil, θ equals the angle of incidence of the electrons with respect to the plane of polarization, and R equals $(1 - \sigma_+/\sigma_-)/(1 + \sigma_+/\sigma_-)$, where σ is the Møller scattering crosssection given by Bincer.[16] The uncertainty in θ contributes less than $\pm 2\%$ error to the final value for P_e. f was measured as described by Ullman[7] and contributes about 4% error. Of these quantities by far the greatest error occurs in δ. For a two month run C_+ can be measured to about 1% accuracy which results in 15% error in δ. At the incident energy of 780 keV P_e was measured to be -1.1 ± 0.2 which is within the assumed theoretical value of -0.92.

The completeness of this error analysis is questionable. First, depolarization of the electrons in the source will be present. Calculations similar to those of Bienlein *et al.*[17] and Mühlschlegel and Koppe[18] indicate a depolarization of 1 to 2% at an energy of 780 keV. Multiple scattering in the target foil is not a problem due to the target's thinness and the method of analysis. Second, a major source of error is introduced by the possibility that the geometry of the aluminum target is not exactly that of the iron target. No direct method was found to avoid this problem.

In order to ascertain the accuracy of the polarization value a second type of measurement was performed. Leaving the iron geometry undisturbed a different source of polarized electrons was measured. ^{137}Cs has a lower energy branch conveniently available so that a comparison was made which introduced no additional source anisotropies. This method removed all use of aluminum for normalization. Assuming a v/c polarization for the low energy 514 keV branch and normalizing the 780 keV data to runs taken at 425 keV resulted in a value of $P_e = -0.89 \pm 0.13$. Again agreement with allowed theory is noted. The second method contains an additional error in that the scattering angle ϕ should be readjusted from 36° to 39° because of the kinematics of the lower energy collision. The correct value of ϕ lies within the width of $\Delta\Phi = \pm 5°$ caused by the collimators. The positions of the detectors were not changed in order to preserve the geometry exactly. At this lower energy depolarization will become a more appreciable source of error.

As a final check on the method of analysis the allowed β decay of ^{32}P was analyzed by the first method (aluminum scattering used for normalization of source anisotropies). The intense high level β branch at 1.71 MeV enabled excellent overlap of energies at 780 keV. The measured value of $P_e = -0.85 \pm 0.17$, without depolarization correction applied, indicates the apparatus is working properly.

The improvement of statistics by means of continued measurement appears futile. Sources of this strength destroy their ultrathin source holders in a time required to obtain results of 15% accuracy for the geometry chosen. This is not a problem for other sources such as ^{32}P but

the studied transition in ^{137}Cs is uniquely difficult because of the low level of intensity and the presence of intense conversion electrons and other decay branches at nearby energies.

The measured value of helicity is consistent with what would be expected for the polarization of electrons from an allowed decay. In forbidden transitions the usually dominant matrix elements may interfere destructively and the electron's polarization may be smaller than $-v/c$. A substantial deviation would not be surprising because of the high forbiddenness in ^{137}Cs, but this deviation has not been observed.

ACKNOWLEDGMENTS

The authors wish to express their gratitude to Professor J. R. Richardson, Professor J. W. Sunier, and Professor H. Appel of the University of California at Los Angeles for their help in the early aspects of this experiment. Graduate students Thomas McPharlin, Joe Swenson, Kenneth Raschke, and Ronald Stagers at California State University, Northridge, also contributed much to the project. The California State University Foundation at Northridge helped by providing aid to obtain the cesium nitrate source.

[1]R.P. Feynmann and M. Gell-Mann, Phys. Rev. 109, 193 (1958).
[2]E. J. Konopinski, Annu. Rev. Nucl. Sci. 9, 99 (1959).
[3]M. Gell-Mann, Rev. Mod. Phys. 31, 834 (1959).
[4]H. A. Tolhoek, Rev. Mod. Phys. 28, 277 (1956).
[5]J. S. Geiger, Phys. Rev. 112, 1684 (1958).
[6]J. S. Greenberg, Phys. Rev. 120, 1393 (1960).
[7]J. D. Ullman, H. Frauenfelder, H. J. Lipkin, and A. Rossi, Phys. Rev. 122, 536 (1961).
[8]V. Eckardt, Phys. Lett. 13, 53 (1964).
[9]P. Lipnik and J. W. Sunier, Phys. Lett. 7, 53 (1963).
[10]P. Lipnik, J. W. Sunier, and A. Pralong, Nucl. Phys. 59, 504 (1964).
[11]H. F. Schopper, *Weak Interactions and Nuclear Beta Decay* (North-Holland, Amsterdam, 1966), pp. 347-348.
[12]C. S. Wu and S. A. Moszkowski, *Beta Decay* (Wiley, New York, 1966), pp. 105-106.
[13]K. Siegbahn, *Alpha-, Beta- and Gamma-Ray Spectroscopy* (North-Holland, Amsterdam, 1965), pp. 1437-1449.
[14]L. Yuan and C. S. Wu, *Methods of Experimental Physics, Nuclear Physics, part B* (Academic Press, New York, 1963), pp. 239-249.
[15]H. L. B. Gould and D. H. Wenny, Elec. Eng. Am. Inst. Electr. Eng. 76, 208 (1957).
[16]A. M. Bincer, Phys. Rev. 107, 1434 (1957).
[17]H. Bienlein, K. Guthner, H. von Issendorf, and H. Wegener, Nucl. Instrum. 4, 87 (1959).
[18]B. Mühlschlegel and H. Koppe, Z. Phys. 150, 474 (1958).